NJC

PAPER

View Article Online
View Journal | View Issue

Stabilizing Pd^{II} on hollow magnetic mesoporous spheres: a highly active and recyclable catalyst for carbonylative cross-coupling and Suzuki coupling reactions†

Cite this: *New J. Chem.*, 2014, **38**, 1471

Received (in Montpellier, France) 18th October 2013,
Accepted 16th December 2013

DOI: 10.1039/c3nj01293j

www.rsc.org/njc

Jianrui Niu, Mengmeng Liu, Peng Wang, Yu Long, Miao Xie, Rong Li* and Jiantai Ma*

A hollow magnetic mesoporous silica sphere (HMMS) catalyst has been synthesized using polystyrene microspheres as a chemical template. The catalyst was characterized by TEM, XRD, XPS and vibrating sample magnetometry (VSM). The catalyst shows high activity for the carbonylative cross-coupling reaction of aryl iodides with arylboronic acids and Suzuki coupling reactions. The newly developed catalyst is easy to recover by magnetic separation from the liquid phase of the reaction and can be recycled. Importantly, the catalyst revealed high efficiency and high stability under the reaction conditions and during recycling stages.

Introduction

The Suzuki coupling reaction has been shown to be an efficient method for the construction of C–C bonds and plays an important role in the pharmaceutical industry and organic synthesis. Furthermore, biaryl ketones are important moieties in many biologically active molecules, natural products and pharmaceuticals. Various methods have been reported for their preparation.[1] Among them, the Suzuki carbonylative coupling reaction is one of the most promising methods for the direct synthesis of biaryl ketones from carbon monoxide, aryl halides and arylboronic acids, since a wide variety of functionalities can be tolerated on either partner and the arylboronic acids are generally nontoxic and thermally-, air- and moisture-stable.[2] To date, Pd catalysts have been widely used in the two reactions.

Nevertheless, one key challenge for the commercial development and practical use of homogeneous Pd-catalysts is the separation of product from the catalytic media. This process is often complicated and usually accomplished by means of complex work-up procedures.[3] To solve these problems and make the process more "green", researchers have immobilized palladium complexes on various supports such as carbon,[4] silica,[5] hydroxyapatite,[6] zeolites[7] and organic polymers[8] to create heterogeneous catalysts. In particular, magnetic nanoparticles have received significant attention and have been widely used in various fields (such as drug delivery,[9] magnetic resonance imaging,[10] biomolecular sensors,[11] bioseparation,[12] and magneto-thermal therapy,[13] catalytic systems[14]), due to the magnetic separation being rapid and highly efficient. What is more, their special magnetic properties allow for quick separation from aqueous systems in the presence of an external magnetic field. To enhance the immobilization of the catalytically active metal on the support's surface, whilst preventing their agglomeration, we always functionalize the magnetic nanoparticles. Compared with amine functionalization, thiol-modified magnetic nanoparticles have a higher affinity for Pd, which was inspired by the work of Fryxell *et al.*[15] and Pinnavaia and Mercier *et al.*,[16] who demonstrated that thiol-modified mesoporous materials are remarkable scavengers for mercury, and by Kang *et al.*,[17,18] who showed that SBA-15-SH has a higher affinity for Pd and Pt compared to other metals.

In the last decade, hollow magnetic mesoporous silica spheres (HMMS) have represented a new class of powerful carrier because of their well-defined structures, uniform size, low density, large surface area, and wide range of potential applications. Compared to the conventional mesoporous silica materials such as MCM-41, SBA-15, FSM-16 and MCF, HMMS have exhibited good catalyst loading properties for confined cooperative catalysis, as they could prevent aggregation of metallic nanoparticles and promote the mass diffusion and transport of reactants. Herein, we present a reusable palladium catalyst with Fe_3O_4 nanoparticles embedded in the mesoporous shell for carbonylative cross-coupling and Suzuki coupling reactions.

College of Chemistry and Chemical Engineering, Lanzhou University, Lanzhou 730000, P. R. China. E-mail: liyirong@lzu.edu.cn, majiantai@lzu.edu.cn; Fax: +86-931-891-2582; Tel: +86-931-891-2311, +86-931-891-3597

† Electronic supplementary information (ESI) available. See DOI: 10.1039/c3nj01293j

Experimental

Synthesis of the hydrophobic magnetite nanoparticles (Fe_3O_4 NPs)

The Fe_3O_4 NPs were prepared using a published method with slight modification.[16] First, 4.8 g of $FeCl_3 \cdot 6H_2O$, 2.0 g $FeCl_2 \cdot 4H_2O$ and 1.0 mL oleic acid were added to 40 mL of deionized water under vigorous stirring. Second, the mixture solution was purged with nitrogen gas for 30 min under nitrogen atmosphere. Third, the mixture solution was heated to 90 °C. Finally, 10 mL of ammonium hydroxide (28 wt%) was added rapidly to the solution, and it immediately turned black. The reaction was kept at 90 °C for 2.5 h. The black precipitate was separated with the help of a magnet and dried at 323 K overnight.

Preparation of polystyrene latex with attached Fe_3O_4 nanoparticles

Briefly, carboxylic polystyrene (PS) latex was prepared by the soap-free emulsion polymerization of styrene (St) with acrylic acid (AA). 1.5 g Fe_3O_4 NPs and 2.5 g negatively charged PS latex were dispersed in 84 mL and 60 mL hydrochloric acid solution (pH = 2.3), respectively. Then the latter suspension was added dropwise into the former under vigorous stirring at room temperature. After 6 h, the heteroaggregates, *i.e.*, Fe_3O_4 NPs attached to the surface of PS latex particles, were separated from the solution by an external magnet and washed several times with water until the pH value of the solution became close to 7.

Preparation of hollow magnetic mesoporous silica spheres (HMMS)

First, 2.0 g heteroaggregate of the PS latex and Fe_3O_4 nanoparticles were dispersed in a solution composed of 75 mL of ethanol, 5 mL of H_2O, and 3.8 mL of $NH_3 \cdot H_2O$ (28 wt%). After stirring for 10 min, 0.4 mL of TEOS and C_{18}TMS mixture with a molar ratio of 4.7 : 1 were added dropwise under vigorous stirring. Then, the reaction proceeded for 8 h at room temperature under stirring. The resultant particles were separated by centrifugation, purified by three cycles of magnetic separation/washing in ethanol, and dried at room temperature for 12 h. Finally, the as-prepared products were dried at 313 K overnight and calcined in air at 823 K for 7 h.

Hollow magnetic mesoporous silica spherical magnetite nanoparticles were synthesized *via* the versatile solvothermal reaction reported by Rong.[24]

Preparation of thiol-modified hollow magnetic mesoporous silica spheres (HMMS-SH)

The functionalization of the HMMS nanoparticles was carried out by adding 0.5 mL mercaptopropyl trimethoxysilane to 200 mL of dry toluene containing 500 mg of HMMS nanoparticles. The resulting solution was refluxed for 24 h and then washed with toluene and acetone. The obtained solid material was dried in vacuum at 50 °C for 24 h.

Loading of Pd on thiol-modified silica coated HMMS (HMMS-SH–Pd^{II})

500 mg of the HMMS-SH sample was first dispersed in a 50 mL ethanol solution under ultrasonication for 0.5 h. The formed black suspension was ultrasonically mixed with 0.188 mmol of a $PdCl_2$ solution for 1 h, then after 2 h of vigorous stirring, the products were obtained with the help of a magnet, washed thoroughly with deionized water and then dried in a vacuum at room temperature overnight.

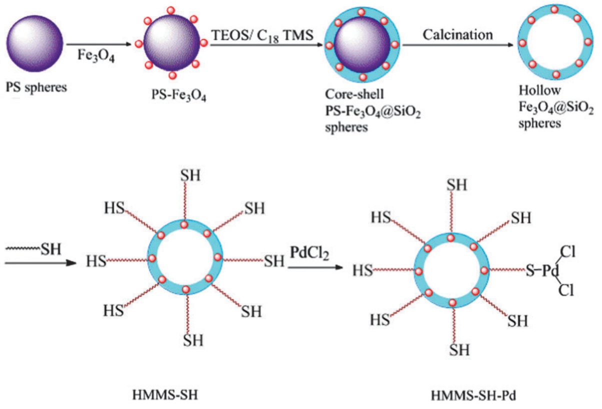

Scheme 1 Preparation of the catalyst.

The preparation of the HMMS-SH–Pd^{II} catalyst follows the steps described in Scheme 1. Firstly, HMMS were prepared. Secondly, the functionalization of the silica coated HMMS with mercaptopropyltrimethoxysilane. Thirdly, under mechanical stirring, palladium chloride was supported on the surface of ligand-modified magnetic nanoparticles.

Typical procedure for the carbonylative Suzuki coupling reactions

A mixture of aryl iodide (0.5 mmol), arylboronic acid (0.6 mmol), K_2CO_3 (1.5 mmol), and 1.5 mol% palladium catalyst in anisole (5 mL) were stirred at 80 °C under 1 atm pressure of CO. The reaction process was monitored by thin layer chromatography (TLC), and the conversion was estimated by GC after separation of the catalyst from the reaction mixture with a magnet. The catalyst was then washed several times with ethanol and dried at room temperature for its reuse.

Typical procedure for the Suzuki coupling reactions

In the Suzuki coupling reactions, 0.5 mmol of aryl halides, 0.7 mmol of phenyl boric acid and 1.5 mmol of base were taken into 5 mL of solvent. The amount of catalyst used in each reaction was 0.6 mol%, and the reaction mixture was refluxed at 343 K. The reaction process was monitored by TLC, and the conversion was estimated by GC after separation of the catalyst from the reaction mixture with a magnet. The catalyst was then washed several times with ethanol and dried at room temperature for its reuse.

Results and discussions

Transmission electron microscopy (TEM) images were obtained using a Tecnai G2F30 transmission electron microscope. The typical TEM image of the catalyst is showed in Fig. 1. As shown in Fig. 1 the average diameter of the as-synthesized spherical particles was about 250 nm and they were nearly monodisperse. A continuous layer of SiO_2 could be observed, and the thickness

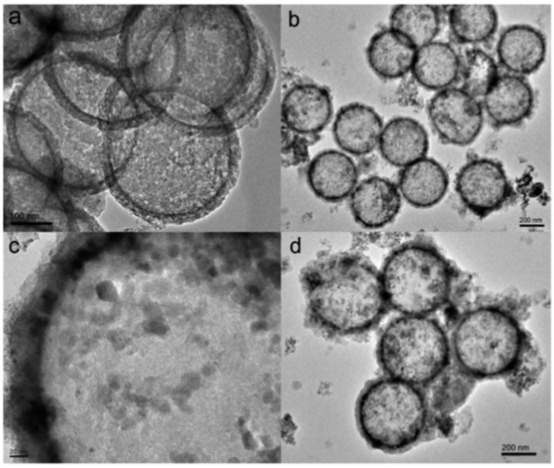

Fig. 1 TEM images of (a) HMMS, (b, c) HMMS-SH and (d) HMMS-SH–Pd^{II}.

is about 30 nm. The TEM in Fig. 1d show that the HMMS-SH–Pd^{II} did not change morphology after $PdCl_2$ coordinated to the surface of the hollow magnetic silica sphere.

X-Ray diffraction (XRD) measurements were performed on a Rigaku D/max-2400 diffractometer using Cu-Kα radiation as the X-ray source in the 2θ range of 20–70°. The XRD pattern of the HMMS (see Fig. 2a) shows characteristic peaks of magnetite nanoparticles and the sharp, strong peaks confirm that the products are well crystallized and the detected diffraction peaks in every pattern could be indexed as cubic Fe_3O_4 (JCPDS card No. 82-1533). In Fig. 2b, the main peaks of the HMMS-SH–Pd^{II} composite were similar to those of the HMMS, which illustrated that the decorating of thiol and immobilization of $PdCl_2$ on the surface of the HMMS did not influence the features of the HMMS.

The X-ray photoelectron spectroscopy (XPS) data was recorded on a PHI-5702 instrument and a C_{1S} line at 292.1 eV was used as the binding energy reference. The XPS elemental survey scans of the surface of the HMMS-SH–Pd^{II} catalyst are shown in Fig. 3. Peaks corresponding to iron, oxygen, sulfur, palladium, silicon and carbon were clearly observed. To ascertain the oxidation state of the Pd, XPS studies were carried out. In Fig. 3b, the Pd binding energy of HMMS-SH–Pd^{II} exhibited two strong peaks centered at 343.8 and 338.4 eV, which were assigned to Pd $3d_{3/2}$ and Pd $3d_{5/2}$, respectively. These values agreed with the Pd^{II} binding energy of $PdCl_2$.

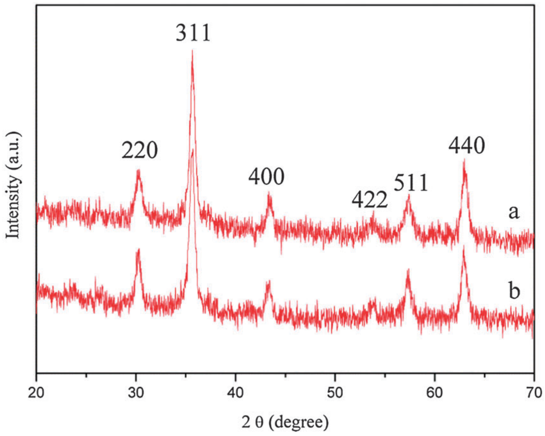

Fig. 2 XRD patterns of (a) HMMS and (b) HMMS-SH–Pd^{II}.

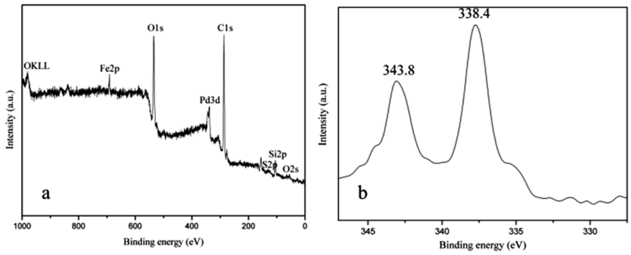

Fig. 3 (a) XPS spectrum of the elemental survey scan of HMMS-SH–Pd^{II} and (b) the XPS spectrum of the HMMS-SH–Pd^{II} showing Pd $3d_{5/2}$ and Pd $3d_{3/2}$ binding energies.

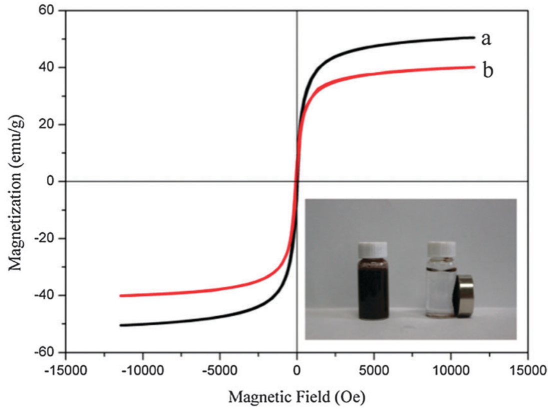

Fig. 4 Magnetization curves of (a) HMMS-SH and (b) HMMS-SH–Pd^{II}.

The magnetic measurements of samples were obtained using a vibrating sample magnetometer (Lake Shore 7304) at room temperature. The magnetization curves measured for HMMS-SH and HMMS-SH–Pd^{II} are compared in Fig. 4, which showed no detectable hysteresis loop, and neither coercivity nor remanence was observed, suggesting that the two nanoparticles are superparamagnetic. Furthermore, it was observed that the saturation magnetizations were 50.53 and 40.08 emu g^{-1} for HMMS-SH and HMMS-SH–Pd^{II}, respectively. The decrease of the saturation magnetization suggests the presence of some palladium particles on the surface of the magnetic support. Even with this reduction in the saturation magnetization, the nanomaterials could still be efficiently separated from the solution by placing a magnet near the reaction vessel.

To explore the optimal reaction conditions, the coupling of iodobenzene with phenylboronic acid was determined in a model reaction (see Table 1). The preliminary results indicated that temperature, base and solvent had a significant effect on the coupling reaction. From Table 1, when the temperature increased from 60 °C to 80 °C, a high yield of the desired product (94%) was obtained (Table 1, entries 1 and 2). However, at an increased temperature of 100 °C (Table 1, entry 3), the yield of the desired product (90%) was decreased, due to the

Table 1 The carbonylative cross-coupling of phenylboronic acid with iodobenzene under different conditions[a]

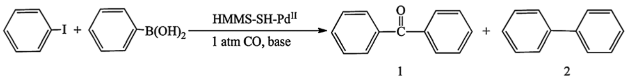

Entry	Solvent	Base	Temp./°C	Time/h	Yield[b] 1	Yield[b] 2
1	Anisole	K_2CO_3	60	9	60	8
2	Anisole	K_2CO_3	80	9	94	3
3	Anisole	K_2CO_3	100	9	90	10
4	Toluene	K_2CO_3	80	9	54	12
5	Dioxane	K_2CO_3	80	9	51	13
6	DMF	K_2CO_3	80	9	68	5
7	Anisole	NaAc	80	9	0	0
8	Anisole	Cs_2CO_3	80	9	8	9
9	Anisole	K_3PO_4	80	9	88	11
10	Anisole	Na_2CO_3	80	9	87	10

[a] The reactions were carried out with iodobenzene (0.5 mmol), arylboronic acid (0.6 mmol), CO (1 atm), base (1.5 mmol), solvent (5 mL), and 1.5 mol% palladium catalyst. [b] Determined by GC.

Table 2 Carbonylative Suzuki coupling reaction of various aryl iodides with arylboronic acids in the presence of the HMMS-SH–Pd^{II} catalyst[a]

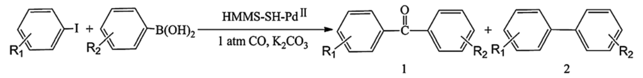

Entry	R_1	R_2	*t*/h	Yield[b] (%) 1	Yield[b] (%) 2	TON	TOF (h^{-1})
1	H	H	9	94	3	62.6	6.96
2	H	4-CH_3	9	87	11.3	58.0	6.44
3	H	4-Cl	9	91	6	60.6	6.73
4	4-CH_3	H	9	91	3.3	60.6	6.73
5	4-CH_3	4-CH_3	9	89	10.1	59.3	6.59
6	4-CH_3	4-Cl	9	85	5	56.7	6.30
7	4-CH_3O	H	9	93	6.7	62.0	6.89
8	4-CH_3O	4-CH_3	9	90	9	60.0	6.67
9	4-CH_3O	4-Cl	9	86	2	57.3	6.37
10	2-NH_2	H	12	95	1.3	63.3	5.28
11	2-NH_2	4-CH_3	12	90	2	60.0	5.00
12	2-NH_2	4-Cl	12	99	0.6	66.0	5.50
13	2-NO_2	H	7	97	0.5	66.0	9.43
14	2-NO_2	4-CH_3	7	97	<0.1	64.7	9.24
15	2-NO_2	4-Cl	7	99	<0.1	66.0	9.43
16	4-CH_3CO	H	7	90	4	60.0	8.57
17	4-CH_3CO	4-CH_3	7	87	12	58.0	8.29
18	4-CH_3CO	4-Cl	7	92	5	61.3	8.76

[a] The reactions were carried out with iodide (0.5 mmol), arylboronic acid (0.6 mmol), CO (1 atm), base (1.5 mmol), solvent (5 mL), and 1.5 mol% palladium catalyst. [b] Determined by GC.

increased amount of the direct coupling product. Therefore, the best temperature was 80 °C. According to the evaluated results of the solvent testing, anisole was found to be the best (Table 1, entries 2 and 4–6). Under the optimized reaction temperature and solvent conditions, several bases were examined, such as NaAc, K_3PO_4, Ce_2CO_3, Na_2CO_3 and K_2CO_3 (Table 1, entries 2 and 7–10). As a result, the most used base K_2CO_3 was the most efficient base to produce carbonylative cross-coupling product. Therefore, the optimized reaction conditions are: 80 °C, anisole, and K_2CO_3.

The reaction mechanism may proceed through a catalytic cycle (see Scheme 2). Oxidative addition of ArI to a Pd^0 complex provides Ar–Pd–I (step 1), which is followed by migratory insertion of carbon monoxide giving ArCO–Pd–I (step 2). Subsequent transmetalation and reductive elimination of the ketone from ArCO–Pd–Ar^1 reproduces the Pd^0 species.[3] In addition, the activity of the palladium-complexes immobilized on HMMS-SH was tested in the Suzuki carbonylative coupling reactions of aryl halides, namely the reactivity of aryl halides with arylboronic acids using K_2CO_3 as a base under balloon pressure of CO in anisole. As shown in Table 2, a variety of arylboronic acids and aryl iodides could proceed smoothly under mild conditions to afford the corresponding carbonylative coupling products in high yields, whether using arylboronic acids and aryl iodides containing either electron-withdrawing groups or electron-donating groups. Yields of the products are almost >90% (Table 2, entries 1–18). It is worth noting that aryl iodides containing electron-withdrawing groups, such as 4-CH_3CO and 2-NO_2 (Table 2, entries 13–18), were found to be the more active (7 h) than aryl iodides containing electron-donating groups (9 h, 12 h), such as 4-CH_3, 4-CH_3O and 2-NH_2 (Table 2, entries 4–12). According to the proposed reaction mechanism, the reason for this could be that the existence of electron-withdrawing groups could promote the oxidative addition of the organic halide to Pd^0 (Scheme 2, step 1). In one word, HMMS-SH–Pd^{II} is an efficient catalyst for carbonylative cross-coupling reactions.

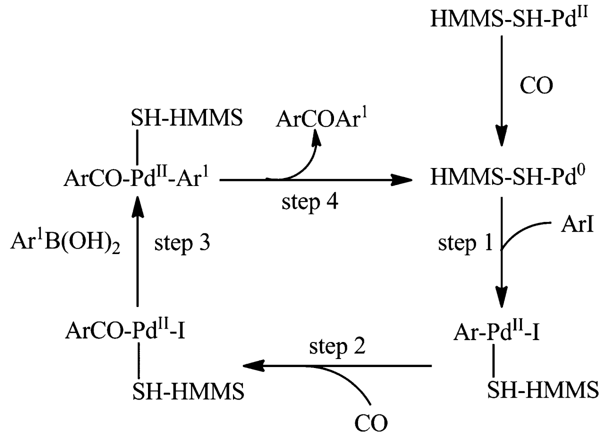

Scheme 2 Reaction mechanism of the carbonylative cross-coupling reaction.

The activity of the HMMS-SH–Pd^{II} catalyst was also investigated for the Suzuki coupling reaction. Table 3 displays the results of the Suzuki cross-coupling reaction of aryl halides with phenylboronic or 4-methylphenylboronic acid. 0.6 mol% of the HMMS-SH–Pd^{II} catalyst afforded satisfactory biaryl yields (97–99%) for aryl bromides with substituents such as $-CH_3$, $-NH_2$, $-COCH_3$ and $-NO_2$, with complete conversions being observed, and the corresponding biaryl products were achieved in 90–99% yields within 45 min–16 h (Table 3). Aryl bromides bearing strong electron-withdrawing groups need a relatively shorter reaction time to obtain a moderate yield (Table 3, entries 6, 7, 10 and 11). Aryl bromides bearing strong electron-donating groups need a relatively longer reaction time in order to obtain a moderate yield (Table 3, entries 4, 5, 8 and 9). Comparing the reactions of bromobenzene and benzyl bromide

Table 3 Suzuki coupling reaction of various arylbromobenzenes with arylboronic acids in the presence of the HMMS-SH–Pd^{II} catalyst[a]

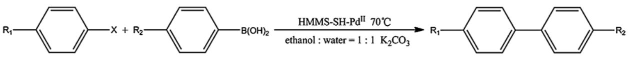

Entry	R_1	X	R_2	*T*	Yield[b] (%)	TON	TOF (h^{-1})
1	H	Br	H	6 h	96	160.3	26.7
2[c]	H	CH_2Br	H	4 h	98	163.3	40.8
3	H	Br	CH_3	8 h	99	165.0	20.6
4	NH_2	Br	H	14 h	95	158.3	11.3
5	NH_2	Br	CH_3	16 h	90	150.0	9.4
6	$COCH_3$	Br	H	60 min	99	165.0	165.0
7	$COCH_3$	Br	CH_3	45 min	98	163.3	217.3
8	CH_3	Br	H	11 h	97	161.7	14.7
9	CH_3	Br	CH_3	14 h	99	165.0	11.8
10	NO_2	Br	H	60 min	98	163.3	163.3
11	NO_2	Br	CH_3	90 min	90	150.0	100.0
12	H	Cl	H	16 h	60	100.0	6.3

[a] The reaction was carried out with 0.5 mmol of arylhalides, 0.7 mmol of phenylboronic acids or 4-methylphenylboronic acid, 1 mmol of K_2CO_3, 0.6 mol% of catalyst and ethanol : water = 1 : 1. [b] Determined by GC or GC-MS. [c] The product was diphenylmethane.

with benzene boric acid (Table 3, entries 1 and 2), the yield of benzyl bromide with benzene boric acid was higher (98%) and the reaction needed a shorter duration (4 h). This is possibly because the Ph–X bond energy (Ph–Br 86.0 kcal mol^{-1}) is generally superior to the corresponding $PhCH_2$–X bond energy ($PhCH_2$–Br 57.2 kcal mol^{-1}).[19]

Further, we investigated the recyclability of the catalyst. After the first reaction cycle, the catalyst was recovered with the help of a magnet, successively washed with distilled water (to remove any excess base) and ethanol, and dried at room temperature ready for the next cycle. The carbonylative cross-coupling reaction of iodobenzene with phenylboronic acid catalyzed by recycled catalyst is displayed in Fig. 5. The weight percentage of Pd in the HMMS-SH–Pd, as determined by atomic absorption spectroscopic (AAS) analysis, was 5.21 wt% before and 4.17% after five cycles.

We compared the results achieved in this work with those reported elsewhere over many other supported catalysts.

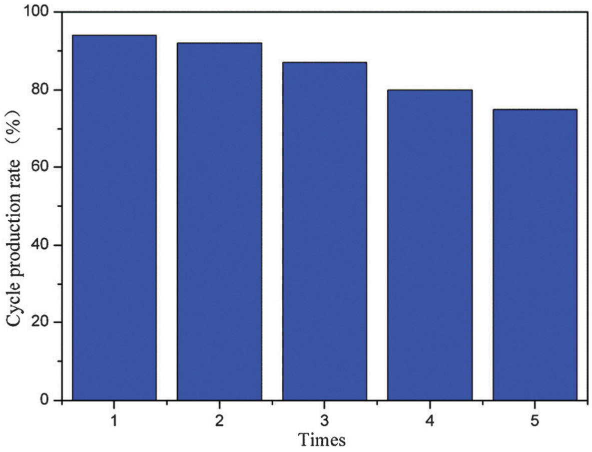

Fig. 5 The yield of the carbonylative cross-coupling reaction of iodobenzene with phenylboronic acid catalyzed by recycled catalyst.

Table 4 The carbonylative cross-coupling of phenylboronic acid with 4-iodoanisole with different catalysts[a]

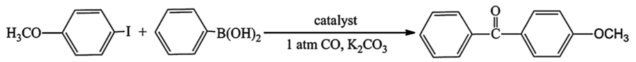

Entry	Catalyst	Catalyst amount (mol%)	Time/h	Temp./°C	Yield (%)
1	MCM-41-2P–Pd^{II}	2	5	80	85
2	Pd/C[b]	2	8	100	85
3	MCM-41-2N–Pd^{II}	2	6	80	86
4	ImmPd–IL[c]	2	8	100	76
5	HMMS-SH–Pd^{II}	1.5	7	80	90

[a] Reaction conditions: CO (1 atm), anisole. [b] Reaction conditions: CO (200 psi), anisole. [c] Reaction conditions: CO (1 MPa), toluene.

Taking the reaction of phenylboronic acid with 4-iodoanisole as an example, the results are listed in Table 4. What is worth mentioning, is that the HMMS-SH–Pd^{II} catalyst displayed an outstanding performance compared with the other heterogeneous catalysts. In contrast with the catalysts of Pd/C[20] and Imm Pd–IL,[21] our catalyst requires a shorter reaction time and milder environment for the carbonylative cross-coupling (Table 4, entries 2, 4 and 5). Although the catalysts of MCM-41-2P–Pd^{II} (ref. 22) and MCM-41-2N–Pd^{II} (ref. 23) gave good yields in a short time and at 80 °C, the amount of Pd consumed is more than that of the HMMS-SH–Pd^{II} catalyst (Table 4, entries 1, 3 and 5).

Conclusion

In conclusion, we combined the advantages of heterogeneous catalysis, magnetic separation and the enhanced catalytic activity of palladium promoted by mercaptopropyl ligands to synthesize a hollow magnetic mesoporous spheres catalyst. In this system, the magnetite nanomaterials play two important roles: one is in increasing the stability of the nanoparticles and the other is preventing Pd(0) leaching during the reaction (due to the presence of surface thiol groups). The catalyst was successfully applied to carbonylative cross-coupling and Suzuki reactions with both high activity and durability.

Acknowledgements

The authors are grateful to the Key Laboratory of Nonferrous Metals Chemistry and Resources Utilization, Gansu Province for financial supports. Additionally, we are also very thankful for the Scholarship Award for Excellent Doctoral Student granted by Lanzhou University.

Notes and references

1 (*a*) N. De. Kimpe, M. Keppens and G. Froncg, *Chem. Commun.*, 1996, 635; (*b*) R. K. Dieter, *Tetrahedron*, 1999, **55**, 4177; (*c*) X.-J. Wang, L. Zhang, X. Sun, Y. Xu, D. Krishnamurthy and C. H. Senanayake, *Org. Lett.*, 2005, **7**, 5593; (*d*) B. Hatano, J. I. Kadokawa and H. Tagaya, *Tetrahedron Lett.*, 2002, **43**, 5859; (*e*) J. F. Hu, Y. P. Wang, M. Han, Y. M. Zhou, X. Q. Jiang and

P. P. Sun, *Catal. Sci. Technol.*, 2012, **2**, 2332; (*f*) M. Han, S. L. Liu, X. P. Nie, D. Yuan, P. P. Sun, Z. H. Dai and J. Ch. Bao, *RSC Adv.*, 2012, **2**, 6061.

2 (*a*) T. Ishiyama, H. Kizaki, T. Hayashi, A. Suzuki and N. Miyaura, *J. Org. Chem.*, 1998, **63**, 4726; (*b*) S. Bonnaire, J. F. Carpentier, A. Mortreux and Y. Castanet, *Tetrahedron Lett.*, 2001, **42**, 3689; (*c*) S. Bonnaire, J. F. Carpentier, A. Mortreux and Y. Castanet, *Tetrahedron*, 2003, **59**, 2793; (*d*) A. Fihri, M. bouhrara, B. Nekoueisharki, J. M. Basset and V. Polshettiwar, *Chem. Soc. Rev.*, 2011, **40**, 5181.

3 M. J. Jacinto, O. H. C. F. Santos, R. F. Jardim, R. Landers and L. M. Rossi, *Appl. Catal., A*, 2009, **2**, 117.

4 (*a*) S. M. Chergui, A. Ledebt, F. Mammeri, F. Herbst, B. Carbonnier, H. B. Romdhane, M. Delamar and M. M. Chehimi, *Langmuir*, 2010, **26**, 16115; (*b*) J. P. Simeone and J. R. Sowa Jr., *Tetrahedron*, 2007, **63**, 12646; (*c*) H. Vijwani and S. M. Mukhopadhyay, *Appl. Surf. Sci.*, 2012, **263**, 712; (*d*) M. Y. Zhu, Y. Wang, C. J. Wang, W. Li and G. W. Diao, *Catal. Sci. Technol.*, 2013, **3**, 952.

5 (*a*) S. Paul and J. H. Clark, *Green Chem.*, 2003, **5**, 635; (*b*) C. M. Crudden, M. Sateesh and R. Lewis, *J. Am. Chem. Soc.*, 2005, **127**, 10045; (*c*) D.-H. Lee, J.-Y. Jung and M.-J. Jin, *Green Chem.*, 2010, **12**, 2024; (*d*) S. Y. Gao, Z. L. Zheng, J. Lü and R. Cao, *Chem. Commun.*, 2010, **46**, 7584; (*e*) Z. Chen, Z. M. Cui, F. Niu, L. Jiang and W. G. Song, *Chem. Commun.*, 2010, **46**, 6524.

6 K. Mori, K. Yamaguchi, T. Hara, T. Mizugaki, K. Ebitani and K. Kaneda, *J. Am. Chem. Soc.*, 2002, **124**, 11572.

7 (*a*) H. Q. Yang, Y. W. Wang, Y. Qin, Y. Z. Chong, Q. Z. Yang, G. Li, L. Zhang and W. Li, *Green Chem.*, 2011, **13**, 1352; (*b*) H. Q. Yang, X. J. Han, Z. C. Ma, R. Q. Wang, J. Liu and X. F. Ji, *Green Chem.*, 2010, **12**, 441; (*c*) H. Q. Yang, Z. C. Ma, Y. Qing, G. Y. Xie, J. Gao, L. Zhang, J. H. Gao and L. Du, *Appl. Catal., A*, 2010, **382**, 312; (*d*) H. Q. Yang, X. J. Han, G. Li and Y. W. Wang, *Green Chem.*, 2009, **11**, 1184; (*e*) X. Feng, M. Yan, T. Zhang, Y. Liu and M. Bao, *Green Chem.*, 2010, **12**, 1758; (*f*) F. Durap, M. Rakap, M. Aydemir and S. Özkar, *Appl. Catal., A*, 2010, **382**, 339; (*g*) J. D. Webb, S. MacQuarrie, K. McEleney and C. M. Crudden, *J. Catal.*, 2007, **252**, 97.

8 (*a*) S. Schweizer, J. Becht and C. L. Drian, *Tetrahedron*, 2010, **66**, 765; (*b*) N. T. S. Phan and P. Styring, *Green Chem.*, 2008, **10**, 1055; (*c*) A. Dahan and M. Portnoy, *J. Am. Chem. Soc.*, 2007, **129**, 5860; (*d*) J. K. Cho, R. Najman, T. W. Dean, O. Ichihara, C. Muller and M. Bradley, *J. Am. Chem. Soc.*, 2006, **128**, 6276; (*e*) B. Atrash, J. Reader and M. Bradley, *Tetrahedron Lett.*, 2003, **44**, 4779; (*f*) R. U. Islam, M. J. Witcomb, M. S. Scurrell, E. Lingen, W. V. Otterlo and K. Mallick, *Catal. Sci. Technol.*, 2011, **1**, 308.

9 (*a*) A. K. Gupta and A. S. G. Curtis, *J. Mater. Sci.: Mater. Med.*, 2004, **15**, 493; (*b*) T. Neuberger, B. Schoepf, H. Hofmann, M. Hofmann and B. V. Rechenberg, *J. Magn. Magn. Mater.*, 2005, **293**, 483.

10 (*a*) B. L. Wang, K. G. Neoh, E. T. Kang, B. Shuter and S.-C. Wang, *Adv. Funct. Mater.*, 2009, **19**, 1; (*b*) Z. Shi, K. G. Neoh, E. T. Kang, B. Shuter, S.-C. Wang, C. Poh and W. Wang, *ACS Appl. Mater. Interfaces*, 2009, **1**, 328.

11 (*a*) J. M. Perez, F. J. Simeone, Y. Saeki, L. Josephson and R. Weissleder, *J. Am. Chem. Soc.*, 2003, **125**, 10192; (*b*) D. L. Graham, H. A. Ferreira and P. P. Freitas, *Trends Biotechnol.*, 2004, **22**, 455.

12 (*a*) D. Wang, J. He, N. Rosenzweig and Z. Rosenzweig, *Nano Lett.*, 2004, **4**, 409; (*b*) C. Xu, K. Xu, H. Gu, R. Zheng, H. Liu, X. Zhang, Z. Guo and B. Xu, *J. Am. Chem. Soc.*, 2004, **126**, 9938.

13 (*a*) R. Hiergeist, W. Andra, N. Buske, R. Hergt, I. Hilger, U. Richter and W. Kaiser, *J. Magn. Magn. Mater.*, 1999, **201**, 420; (*b*) A. Jordan, R. Scholz, P. Wust, H. Fahling and R. Felix, *J. Magn. Magn. Mater.*, 1999, **201**, 413.

14 (*a*) S. Shylesh, V. Schünemann and W. R. Thiel, *Angew. Chem., Int. Ed.*, 2010, **49**, 3428; (*b*) U. Laska, C. G. Frost, G. J. Price and P. K. Plucinski, *J. Catal.*, 2009, **268**, 318; (*c*) H. Q. Yang, G. Li and Z. C. Ma, *J. Mater. Chem.*, 2012, **22**, 6639.

15 X. Feng, G. E. Fryxell, L. Q. Wang, A. Y. Kim, J. Liu and K. M. Kemner, *Science*, 1997, **276**, 923.

16 L. Mercier and T. J. Pinnavaia, *Adv. Mater.*, 1997, **9**, 500.

17 T. Kang, Y. Park, J. C. Park, Y. S. Cho and J. Yi, *Stud. Surf. Sci. Catal.*, 2003, **146**, 527.

18 T. Kang, Y. Park and J. Yi, *Ind. Eng. Chem. Res.*, 2004, **43**, 1478.

19 P. Wang, F. w. Zhang, Y. Long, R. Li and J. T. Ma, *Catal. Sci. Technol.*, 2013, **3**, 1618.

20 M. V. Khedkar, P. J. Tambade, Z. S. Qureshi and B. M. Bhanage, *Eur. J. Org. Chem.*, 2010, 6981.

21 M. V. Khedkar, T. Sasaki and B. M. Bhanage, *RSC Adv.*, 2013, **3**, 7791.

22 M. Z. Cai, G. M. Zheng, L. F. Zha and J. Peng, *Eur. J. Org. Chem.*, 2009, 1585.

23 M. Z. Cai, J. Peng, W. Y. Hao and G. D. Ding, *Green Chem.*, 2011, **13**, 190.

24 L. Y. Xia, M. Q. Zhang, C. Yuan and M. Z. Rong, *J. Mater. Chem.*, 2011, **21**, 9020.